# Towards a fully automatic processing chain for operationally mapping burned areas countrywide exploiting Sentinel-2 imagery

Dimitris Stavrakoudis*[a], Thomas Katagis[a], Chara Minakou[a], Ioannis Z. Gitas[a]
[a] Laboratory of Forest Management and Remote Sensing, School of Forestry and Natural Environment, Aristotle University of Thessaloniki, P.O. Box 248, GR-54124, Greece

## ABSTRACT

Burned area mapping is essential for quantifying the environmental impact of wildfires, for compiling statistics, and for designing effective short- to mid-term impact mitigation measures. The Sentinel-2 satellites are providing an unparalleled wealth of high-resolution remotely sensed information with a short revisit cycle, which is ideal for mapping burned areas both accurately and timely. However, the high detail and volume of the information provided actually encumbers the automation of the mapping process, at least for the level of automation required to map systematically wildfires on a national level. This paper presents a preliminary methodology for mapping burned areas using Sentinel-2 data, which aims to eliminate user interaction and achieve mapping accuracy that is acceptable for operational use. It follows an object-based image analysis (OBIA) approach, whereby the initial image is segmented into a set of adjacent and non-overlapping small regions (objects). The most unambiguous of them are labeled automatically through a set of empirical rules that combine information extracted from both a pre-fire Sentinel-2 image and a post-fire one. The burned area is finally delineated following a supervised learning approach, whereby a Support Vector Machine (SVM) is trained using the labeled objects and subsequently applied to the whole image considering a set of optimally selected object-level features. Preliminary results on a set of recent large wildfires in Greece indicate that the proposed methodology constitutes a solid basis for fully automating the burned area mapping process.

**Keywords:** Operational burned area mapping, object-based image analysis (OBIA), quick shift segmentation, Sentinel-2, automatic training patterns classification, machine learning

## 1. INTRODUCTION

Wildfires constitute an important pressure in forested ecosystems, introducing a high risk of direct damage to humans and structures in most of the highly populated Mediterranean countries and especially in coastal regions[1]. In Europe, about 65,000 fires occur every year on average, burning approximately half a million hectares of wildland and forest areas; most of the burned area—over 85%—is in the European Mediterranean region[2]. The analyses performed by the European Forest Fire Information System (EFFIS) indicate an increase in the length of the wildfire season the last 30 years, whereas the fire regime is projected to change almost everywhere in Europe the next decades[3].

Timely and accurate burned area mapping is essential for quantifying the environmental impact of wildfires, for compiling statistics, and for designing effective short- to mid-term impact mitigation measures (e.g., prevention of soil erosion or possible impacts of the fire/heavy rainfall combination). Satellite imagery has been successfully employed for mapping burned areas for several decades, since it offers a more accurate, seasonable, and resource-efficient alternative to field surveys[4]. Traditionally, moderate- to coarse-resolution satellite sensors have been used for the tasks, such as MODIS (Moderate Resolution Imaging Spectroradiometer)[5] and MERIS (MEdium Resolution Imaging Spectrometer)[6]. These sensors offer the advantage of daily (or sub-daily) global coverage and the possibility to identify the date of the fire through a fully automated workflow. However, their coarse spatial resolution (pixel size of 500 m or greater) provides only a rough estimate of the burn perimeter.

*jstavrak@auth.gr; phone +30 2310 992689; fax +30 2310 992677; http://fmrs.web.auth.gr

Burned area mappings with the detail required by local forest managers can be produced with high-resolution satellite imagery. Landsat data have been predominately used for this purpose[7–9], due to their rich spectral information—especially the shortwave infrared (SWIR) bands they include that are important for burned area mapping—and their free data provision policy from the United States Geological Survey (USGS) since 2008. However, Landsat's temporal resolution of 16 days encumbers the rapid mapping of wildfires, especially in regions with frequent cloud coverage (e.g., mountainous areas). Rapid and detailed mapping can be performed alternatively with commercial very high-resolution satellite imagery[10,11], but this option involves high costs especially if expedited satellite tasking is requested, which limits its applicability to few cases of special significance (e.g., when extended damages are involved).

The Sentinel-2 mission—developed and operated by the European Space Agency (ESA) as part of the Copernicus programme of the European Commission (EC)—is providing free of charge high-resolution optical imagery since 2015. Sentinel-2 data are characterized by high spatial resolution (10–20 m, depending on the band), rich spectral information (more or less a superset of Landsat 7 ETM+ and Landsat 8 OLI bands), and high temporal frequency (5 days), characteristics which constitute them attractive for setting up an operation burned area mapping service on a national level. Since the Sentinel-2 data are new, though, only few studies have investigated their potential for burned area mapping[12–14] and even fewer have proposed automated workflows for automated mapping[15].

The present study's objective is to present a preliminary methodology for mapping burned areas using Sentinel-2 data, which aims to eliminate user interaction and achieve mapping accuracy that is acceptable for operational use. The proposed methodology is based on a previous method, namely, the Object-based Burned Area Mapping (OBAM) service, developed within the context of the Greek National Observatory of Forest Fires (NOFFi)[16]. In brief, NOFFi-OBAM is a semi-automated methodology that uses a single post-fire Sentinel-2 image, following the object-based image analysis (OBIA) approach, that is, the initial image is segmented into a set of adjacent and non-overlapping small regions (objects) and each object is classified as a whole into burned or unburned. The classification is performed by means of a supervised classifier trained with a small set of training objects, which are automatically selected but need to be labeled by the user manually (through photointerpretation). Although the methodology was empirically found to achieve high accuracy and was operationally employed to map more than 150 wildfire in Greece from 2016 to 2018, the manual labeling of the training object can become time-consuming, especially in sparsely vegetated areas and for large wildfires. Hence, the aim of this study is to automate the latter process, exploiting the additional information provided by a pre-fire Sentinel-2 image.

## 2. DATASETS

The proposed methodology uses Sentinel-2 MultiSpectral Instrument (MSI) data. We did not consider the bands with spatial resolution of 60 m—which are primarily useful for atmospheric correction—neither the two additional red edge bands (bands 5 and 7), which are primarily used for indices sensitive to vegetation stress. The nominal specifications[17] of the eight bands that were ultimately considered in this study are reported in Table 1.

Table 1. Sentinel-2 MSI bands considered and their nominal specifications.

| Band | Description | Spatial Resolution (m) | Central wavelength (nm) | Bandwidth (nm) |
|---|---|---|---|---|
| B02 | Blue | 10 | 490 | 65 |
| B03 | Green | 10 | 560 | 35 |
| B04 | Red | 10 | 665 | 30 |
| B06 | Red edge | 20 | 740 | 15 |
| B08 | Near infrared (NIR) | 10 | 842 | 115 |
| B8A | NIR narrow | 20 | 865 | 20 |
| B11 | SWIR 1 | 20 | 1610 | 90 |
| B12 | SWIR 2 | 20 | 2190 | 180 |

Six wildfire events in 2016 and 2018 in Greece were considered in this study (Table 2 and Figure 1), selected to cover representative cases of the Greek ecosystems and to present challenges in burned area mapping. More specifically, Elata (Figure 1a) was a sparsely vegetated environment with many plantations of mastic trees (*Pistacia lentiscus*). In Farakla (Figure 1b), the wildfire burned a dense pine forest and reached urban areas across the coastline. Saktouria (Figure 1c) is a typical Cretan environment, with very sparse low vegetation in mostly rocky areas, which are typically difficult to differentiate from burned areas. Zemeno (Figure 1d) is a mountainous area with rough terrain and several agricultural

fields within the burn perimeter. Finally, Kallitechnoupoli (Figure 1e) and Kineta (Figure 1f) are the two devastating wildfires of 2018 in Attica, where the fire expanded to populated areas with significant vegetation cover (mostly pine trees in-between houses and within house yards).

Table 2. Wildfire events in Greece considered in this study.

| Location | Region | Fire start date | Pre-fire image date | Post-fire image date | Sentinel-2 tile |
|---|---|---|---|---|---|
| Elata | Chios | 23/07/2016 | 20/07/2016 | 27/07/2016 | T35SMC |
| Farakla | Euboea | 30/07/2016 | 23/07/2016 | 02/08/2016 | T34SGH |
| Saktouria | Crete | 30/07/2016 | 27/07/2016 | 06/08/2016 | T35SKU |
| Zemeno | Corinthia | 23/07/2018 | 13/07/2018 | 28/07/2018 | T34SFH |
| Kallitechnoupoli | Attica | 23/07/2018 | 05/07/2018 | 04/08/2018 | T34SGH |
| Kineta | Attica | 23/07/2018 | 13/07/2018 | 14/08/2018 | T34SFH |

We used Level-2A products, that is, atmospherically corrected Sentinel-2 images (bottom-of-atmosphere reflectance values)[18]. The 2018 images were downloaded directly as Level-2A products from the Copernicus Open Access Hub (https://scihub.copernicus.eu/). For the 2016 images, the Sen2Cor processor (http://step.esa.int/main/third-party-plugins-2/sen2cor/) was run locally to derive the Level-2A products. A rectangular subset of the image that includes the burned area with a small buffer around was cropped out of each original Sentinel-2 tile, as shown in Figure 1. In the current work, this was done manually, although we presently explore ways to automate this step as well. The bands reported in Table 1 were subsequently stacked into a single image, considering absolute reflectance values in the range [0,1] (i.e., dividing the Level-2A product's pixel values with 10,000). For this purpose, all 20 m resolution images were resampled to 10 m. Moreover, non-land areas were masked out using the official NUTS (Nomenclature of Territorial Units for Statistics) layer.

For validation purposes, the burn area perimeters derived from the previously mentioned NOFFi-OBAM service were used. Although these mappings were derived from a semi-automated methodology based on the post-fire Sentinel-2 images, manual corrections were performed at the end through careful photointerpretation. Ideally, a proper validation framework would require the reference perimeters to have been derived from images of much higher spatial resolution than that of Sentinel-2. Lacking such data, though, the aforementioned manually corrected reference set is the most accurate reference we could produce, but it is generally accurate in absolute terms considering that Sentinel-2's resolution is high enough to support the photointerpretation process.

## 3. METHODOLOGY

Figure 2 depicts the workflow of the proposed methodology. The post-fire Level-2A image is segmented and the resulting objects are used as the new mapping units of the analysis. Spectral indices are calculated from both the pre-fire and the post-fire image and their difference (or ratio) is used to label automatically a subset of objects by means of empirical rules, thus formulating the training set. These rules are defined in a way such as only objects that can be characterized unambiguously as burned or unburned are labeled, in order to avoid introducing misclassifications into the training set as much as possible. Object-level features are calculated from various sources (post-fire image bands and spectral indices, as well as the differenced spectral indices) and the training set drives the subsequent supervised learning part of the methodology. The latter comprises a feature selection process followed by the classification model construction, out of which the final burned area mapping is obtained. The rest of this section describes each step in detail.

### 3.1. Image segmentation

An image segmentation algorithm partitions the image into a set of adjacent and non-overlapping small regions (segments or objects) considering a homogeneity criterion, although other supplementary criteria such as shape or size can be considered. The homogeneity of the segments versus their size is controlled by one or more parameters that determine the scale of the segmentation (i.e., how fine or coarse the final segmentation is). Conceptually, the OBIA approach tries to derive objects that approximate the natural objects of the scene as perceived by humans[19]. In the proposed methodology, the image segmentation step is applied for a) reducing the computational complexity of the subsequent supervised learning steps and b) avoiding the salt-and-pepper phenomenon frequently encountered in pixel-based classifications. After all, the concept of well-defined natural objects in forested burned areas is fuzzy even for humans. Therefore, we prefer to segment

the image into small and highly homogeneous objects (called over-segmentation in image processing terminology), in order to avoid misclassifying larger regions due to mixed objects.

In order to achieve the aforementioned goal, we employ a superpixel segmentation algorithm, namely the quick shift algorithm[20]. Quick shift is a kernelized mode-seeking clustering algorithm similar to the well-known mean shift[21], but considerably faster. Segmentation is performed on the post-fire image and considering only on the 10 m bands (Blue, Green, Red, and NIR in Table 1). The scale of the segmentation is controlled by a threshold parameter $\tau$ that determines the maximum spectral distance allowed for two sample points (pixels in our case) to be merged into a single cluster. Moreover, the width $\sigma$ of the Gaussian kernel must be defined by the user. In order to identify common values of these two parameters for all cases, we employ a simple image enhancement processing procedure on the four image bands. Specifically, if $f_{i,1\text{st}}$ is the 1% percentile of the *i*th band's histogram and $f_{i,99\text{th}}$ is the equivalent 99% percentile, the image is saturated in the range $[f_{i,1\text{st}}, f_{i,99\text{th}}]$, linearly scaled to the range [1,255], rounded to the nearest integer, and stored in 8-bit format (0 is reserved to represent no-data/masked out areas). This is a typical image enhancement technique used to visualize remote sensing images (actually all pseudo-color views of Figure 1 have been produced this way), since the remote sensing sensors have a much broader intensity range than typical cameras to avoid saturation over very bright objects. The latter are however not important in our case (they are non-burned objects anyway) and can be safely saturated. Applying this processing step, we empirically determined that the values $\tau = 2$ and $\sigma = 1$ for quick shift's parameters provided satisfactory results (i.e., highly homogeneous small objects) in all cases. Figure 3 provides an example of the segmentation scale, considering the case of the Saktouria wildfire (Figure 1c); similarly small objects were produced for all test cases.

The derived objects are then used as the new elementary units for all further processes. The new object-level feature values are the average values of all pixels contained in each image object.

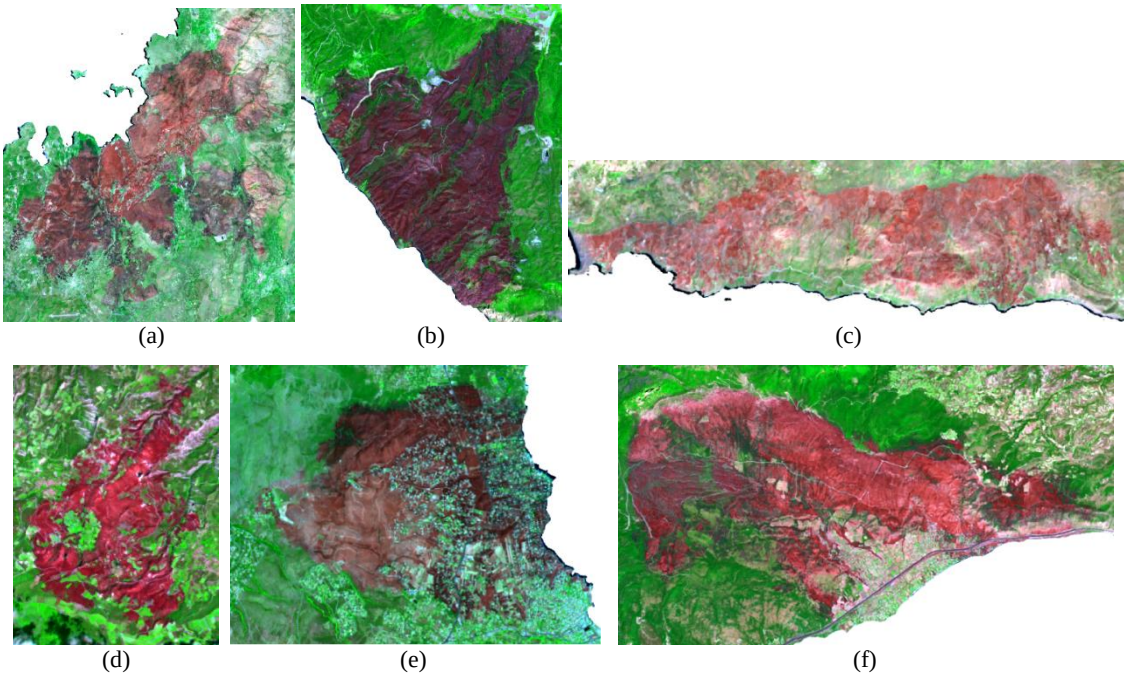


Figure 1. False-color composites (using B12, B08, and B04 in lieu of the view's red, green, and blue channels, respectively) of the post-fire Sentinel-2 images used for each wildfire event: (a) Elata, (b) Farakla, (c) Saktouria, (d) Zemeno, (e) Kallitechnoupoli, and (f) Kineta. Non-land areas have been masked out.

### 3.2. Spectral indices

Apart from the Sentinel-2 bands (Table 1), a number of spectral indices frequently used in burned area mapping studies have been calculated, which are reported in Table 3. Most of them employ the classical normalized difference formulation of NDVI, but using one or both of the SWIR bands, which are sensitive to moisture content and consequently facilitate the discrimination of the burned areas. The indices are calculated considering the ground reflectance values of the Level-2A

products in the range [0,1], from either the pre-fire image or the post-fire one or both (as described in the following subsections). In the following, we use the notation $SI_{pre}$ and $SI_{post}$ to describe any index $SI$ calculated from the pre-fire or the post-fire image, respectively (e.g., $NDVI_{pre}$). Moreover, the empirical rule-based classification (described in the next subsection) also considers the difference between the pre-fire and post-fire values for some of the indices, which is an indication of disturbance resulting from the fire. The difference, which is denoted as d$SI$ for any index $SI$ (e.g., dNBR), is calculated as pre-fire minus post-fire value, that is, $dSI = SI_{pre} - SI_{post}$.

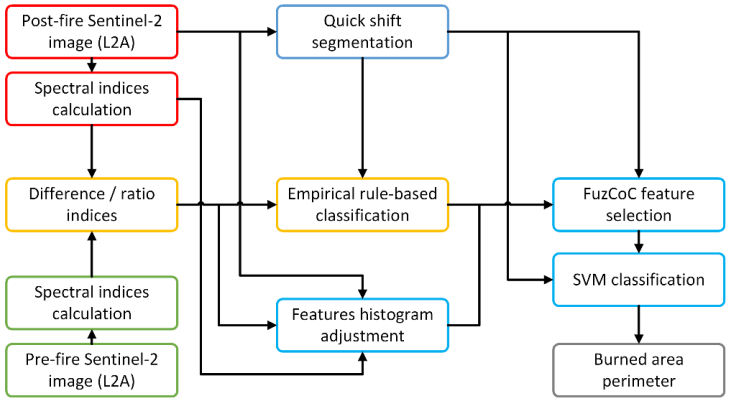


Figure 2. Schematic workflow of the proposed methodology.

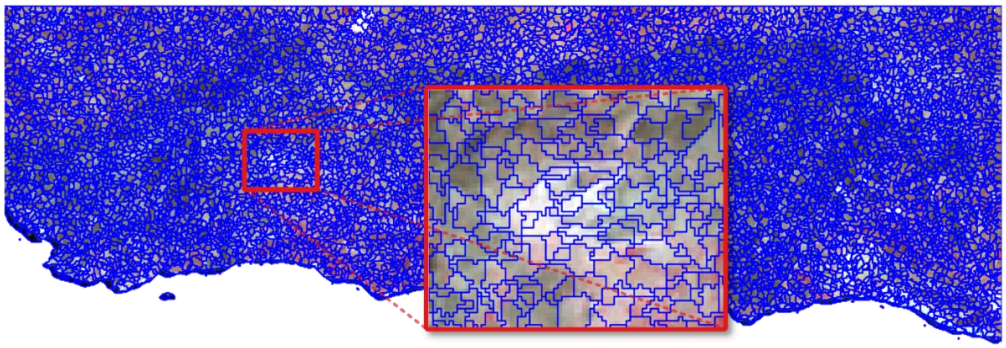

Figure 3. Example of quick shift segmentation scale, considering the case of the Saktouria, Crete wildfire (background Sentinel-2 pseudo-color uses bands B08, B04, and B03 in lieu of RGB).

Table 3. Spectral indices considered in this study. Band names are those reported in Table 1.

| Acronym | Name | Equation | Introduced in |
|---|---|---|---|
| NDVI | Normalized difference vegetation index | (B8A – B04) / (B8A + B04) | Rouse *et al.*[22] |
| MSAVI2 | Modified soil-adjusted vegetation index 2 | $0.5 \cdot \{2 \cdot B8A+1 - \sqrt{(2 \cdot B8A+1)^2 - 8 \cdot (B8A-B04)}\}$ | Qi *et al.*[23] |
| CSI | Char soil index | B8A / B12 | Smith *et al.*[24] |
| MIRBI | Mid-infrared burn index | 10·B12 – 9.8·B11 + 2 | Trigg and Flasse[25] |
| NBR | Normalized burn ratio | (B8A – B12) / (B8A + B12) | Key and Benson[26] |
| NBR2 | Normalized burn ratio 2 | (B11 – B12) / (B11 + B12) | USGS[27] |
| NDII | Normalized difference infrared index | (B8A – B11) / (B8A + B11) | Hardisky[28] |
| MNDWI | Modified normalized difference water index | (B03 – B11) / (B03 + B11) | Xu[29] |

### 3.3. Empirical rule-based classification

As mentioned previously, the supervised classification approach followed by the proposed methodology requires a training set that is labeled automatically. To do so, we defined two empirical rules that employ thresholds on differences or ratios of pre-fire and post-fire indices, following a similar approach with previous studies[8,15]. The threshold values were determined empirically through a trial-and-error procedure on many wildfire events in Greece, in a way that only

unambiguous burned or unburned objects were labeled, in order to avoid introducing errors within the training set. Eventually, an object is classified as burned if it satisfies the rule:

$$\mathrm{MNDWI_{pre}} < -0.3 \; \textit{AND} \; [(\mathrm{B8A_{ratio}} > 0.3 \; \textit{OR} \; \mathrm{dMIRBI} < -1.5) \; \textit{AND} \; \mathrm{dNDII} > 0.02], \quad (1)$$

where

$$\mathrm{B8A_{ratio}} = \mathrm{B8A_{pre}} / \mathrm{B8A_{post}} - 1. \quad (2)$$

Accordingly, an object is classified as unburned if it satisfies the rule:

$$\mathrm{MNDWI_{pre}} > -0.25 \; \textit{OR} \; [\mathrm{dNBR} < -0.015 \; \textit{OR} \; \mathrm{dNBR2} < -0.015]. \quad (3)$$

In both cases, the pre-fire MNDWI index is considered for discriminating water surfaces and artificial areas (buildings, roads, etc.), whereas the vegetation or burned area identification is performed by the remaining part of the corresponding rule. For each object, the feature value considered for employing the rules is the average value of all pixels within the object for the specific feature. Depending on the area, a larger or smaller proportion of objects may be classified by the above rules. Densely vegetated forest areas or severely burned areas are more likely to be labeled. In any case, the labeled objects are used to formulate the training set and the remaining are categorized by the supervised classifier, as explained in the following.

### 3.4. Supervised learning and burned area perimeter delineation

The dataset used for the supervised classification considers 21 potential features extracted from multiple sources. More specifically, it is formulated considering:

1) the eight bands of the post-fire Sentinel-2 image reported in Table 1,
2) the first seven spectral indices of Table 3 calculated from the post-fire image ($\mathrm{NDVI_{post}}$, $\mathrm{MSAVI2_{post}}$, $\mathrm{CSI_{post}}$, $\mathrm{MIRBI_{post}}$, $\mathrm{NBR_{post}}$, $\mathrm{NBR2_{post}}$, and $\mathrm{NDII_{post}}$), and
3) all features considered in the empirical rules of equations (1)–(3) ($\mathrm{B8A_{ratio}}$, dMIRBI, dNDII, dNBR, dNBR2, and $\mathrm{MNDWI_{pre}}$).

The average value of each feature for all pixels within each object was considered for defining the object-level features. The histogram enhancement procedure considered for the segmentation step (Subsection 0) was also applied in this dataset as well. Specifically, each feature was saturated in the range defined by the 1% and 99% percentiles of its histogram, then linearly scaled to the range [1,255], rounded to the nearest integer, and stored in 8-bit format (0 is reserved to represent no-data/masked out areas).

The number of potential features is relative large, which can have a negative effect in the performance of the supervised classifier and increases its computational requirements, especially taking into consideration that in some cases the number of automatically labeled objects is large. In order to select the minimum optimal set of features, we employ the supervised feature selection method based on the fuzzy complementary criterion (FuzCoC)[30]. FuzCoC iteratively adds into the selected set the feature that provides the maximum additional contribution to the previously selected set of features. The process stops when the additional contribution—quantified through an efficient normalized measure—drops below a user-defined threshold, which was set to 0.1% in our experiments. With this threshold value, 6.6 features on average were selected in our six test cases.

Having defined the feature set and the training set from the previous step, a Support Vector Machine (SVM) classification model[31] is learned subsequently, considering a Gaussian kernel. The penalty constant $C$ and the Gaussian kernel's width $\sigma$ are optimized by a 5-fold cross-validation approach on all possible combinations for the two parameters, considering an exponentially increasing grid of possible values for each parameter. The trained SVM model is subsequently applied to classify all objects and the final burned area map is derived by keeping only the objects classified as burned and merging them into a single object (vector map).

## 4. RESULTS

As mentioned in Section 0, manually corrected fire perimeters from the NOFFi-OBAM service were used as reference data. For quantifying accuracy, well-known measures derived from the confusion matrix were calculated, namely, sensitivity, specificity, precision, accuracy, and F-measure[32]. Table 4 reports the accuracy measures values achieved by

the proposed method for the six test cases presented in Section 0. Moreover, Figure 4 presents a visual comparison of the reference perimeter and that obtained by the proposed method.

Overall, the proposed methodology exhibits high accuracy, with almost all individual measure values being higher or much higher than 90%. In most cases, the proposed method seems to underestimate the burned area within the fire perimeter, which is most notably observed in the case of Kineta (Figure 4f), but also in the cases of Saktouria (Figure 4c) and Kallitechnoupoli (Figure 4e). This is also reflected by the somewhat lower sensitivity values for these datasets (Table 4). In the cases of Kineta and Kallitechnoupoli, the unburned misclassifications result from residential areas with partially burned vegetation, which are characterized by mixed objects and hence no training patterns exist (the empirical rules label only unambiguous objects). In the case of Saktouria, the unburned misclassification are the result of the sparsely vegetated areas before the burn, which make it difficult to discriminate from burned areas. On the contrary, a slight overestimation of the burned area is observed in the case of Zemeno, which is also reflected by the somewhat lower values of specificity and precision measures. This is a small proportion of the burned area though, as proved by the high sensitivity and accuracy values.

Table 4. Accuracy measures values obtained by the proposed methodology.

| Area | Sensitivity | Specificity | Precision | Accuracy | F-measure |
|---|---|---|---|---|---|
| Elata | 0.94 | 0.97 | 0.96 | 0.96 | 0.95 |
| Farakla | 0.99 | 0.94 | 0.94 | 0.96 | 0.97 |
| Saktouria | 0.89 | 0.97 | 0.96 | 0.93 | 0.92 |
| Zemeno | 0.98 | 0.90 | 0.83 | 0.93 | 0.90 |
| Kallitechnoupoli | 0.95 | 0.95 | 0.96 | 0.95 | 0.95 |
| Kineta | 0.84 | 0.99 | 0.99 | 0.92 | 0.91 |

## 5. CONCLUSIONS

This paper presented a preliminary methodology for mapping burned areas using Sentinel-2 data without any user interaction. This is achieved by automatically labeling a set of training patterns by means of a set of empirical rules that combine information extracted from both a pre-fire Sentinel-2 image and a post-fire one, whereas the rest of the image is classified following a supervised learning approach. The results on a set of recent large wildfires in Greece showed that the methodology achieves satisfactory performance, considering the fact that it is a fully automated process. Future research will focus on (a) refining the set of empirical rules to cover difficult mapping cases (residential areas with high vegetation cover, sparsely vegetated areas, etc.), (b) automate the wildfire event identification process, and (c) employ semi-supervised learning procedures to enhance the automatic labeling of training objects.

## ACKNOWLEDGEMENTS

This research is funded in the context of the project “Development of advanced algorithm and open-source software for automated burned area mapping using high-resolution data” (MIS 5005537) under the call for proposals “Supporting researchers with emphasis on new researchers” (EDULLL 34). The project is co-financed by Greece and the European Union (European Social Fund – ESF) by the Operational Programme “Human Resources Development, Education and Lifelong Learning 2014-2020”.

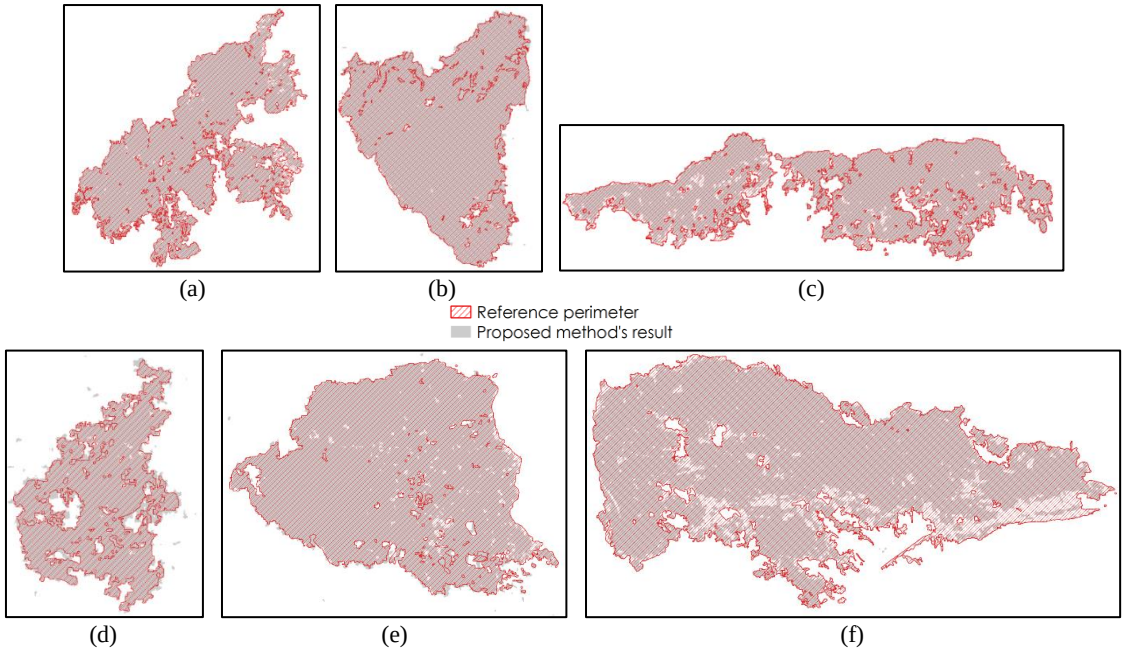


Figure 4. Comparison of the proposed method's burned area mapping with the reference perimeter for the wildfire event of: (a) Elata, (b) Farakla, (c) Saktouria, (d) Zemeno, (e) Kallitechnoupoli, and (f) Kineta.

## REFERENCES


[1] Pausas, J. G., Llovet, J., Rodrigo, A. and Vallejo, R., "Are wildfires a disaster in the Mediterranean basin? – A review," Int. J. Wildland Fire 17(6), 713–723 (2009).

[2] San-Miguel-Ayanz, J., Moreno, J. M. and Camia, A., "Analysis of large fires in European Mediterranean landscapes: Lessons learned and perspectives," For. Ecol. Manag. 294, 11–22 (2013).

[3] San-Miguel-Ayanz, J., Durrant, T., Boca, R., Libertà, G., Branco, A., Rigo, D. de, Ferrari, D., Maianti, P., Vivancos, T. A., Costa, H., Lana, F., Löffler, P., Nuijten, D., Ahlgren, A. C. and Leray, T., "Forest Fires in Europe, Middle East and North Africa 2017," EUR 29318 EN, Publications Office of the European Union, Luxembourg (2018).

[4] Chuvieco, E., Mouillot, F., van der Werf, G. R., San Miguel, J., Tanase, M., Koutsias, N., García, M., Yebra, M., Padilla, M., Gitas, I., Heil, A., Hawbaker, T. J. and Giglio, L., "Historical background and current developments for mapping burned area from satellite Earth observation," Remote Sens. Environ. 225, 45–64 (2019).

[5] Giglio, L., Boschetti, L., Roy, D. P., Humber, M. L. and Justice, C. O., "The Collection 6 MODIS burned area mapping algorithm and product," Remote Sens. Environ. 217, 72–85 (2018).

[6] Chuvieco, E., Yue, C., Heil, A., Mouillot, F., Alonso-Canas, I., Padilla, M., Pereira, J. M., Oom, D. and Tansey, K., "A new global burned area product for climate assessment of fire impacts," Glob. Ecol. Biogeogr. 25(5), 619–629 (2016).

[7] Goodwin, N. R. and Collett, L. J., "Development of an automated method for mapping fire history captured in Landsat TM and ETM + time series across Queensland, Australia," Remote Sens. Environ. 148, 206–221 (2014).

[8] Bastarrika, A., Alvarado, M., Artano, K., Martinez, M. P., Mesanza, A., Torre, L., Ramo, R. and Chuvieco, E., "BAMS: A Tool for Supervised Burned Area Mapping Using Landsat Data," Remote Sens. 6(12), 12360–12380 (2014).

[9] Hawbaker, T. J., Vanderhoof, M. K., Beal, Y.-J., Takacs, J. D., Schmidt, G. L., Falgout, J. T., Williams, B., Fairaux, N. M., Caldwell, M. K., Picotte, J. J., Howard, S. M., Stitt, S. and Dwyer, J. L., "Mapping burned areas using dense time-series of Landsat data," Remote Sens. Environ. 198, 504–522 (2017).

[10] Dragozi, E., Gitas, I. Z., Stavrakoudis, D. G. and Theocharis, J. B., "Burned Area Mapping Using Support Vector Machines and the FuzCoC Feature Selection Method on VHR IKONOS Imagery," Remote Sens. 6(12), 12005–12036 (2014).

[11] Sertel, E. and Alganci, U., "Comparison of pixel and object-based classification for burned area mapping using SPOT-6 images," Geomat. Nat. Hazards Risk 7(4), 1198–1206 (2016).
[12] Huang, H., Roy, D. P., Boschetti, L., Zhang, H. K., Yan, L., Kumar, S. S., Gomez-Dans, J. and Li, J., "Separability Analysis of Sentinel-2A Multi-Spectral Instrument (MSI) Data for Burned Area Discrimination," Remote Sens. 8(10), 873 (2016).
[13] Fernández-Manso, A., Fernández-Manso, O. and Quintano, C., "SENTINEL-2A red-edge spectral indices suitability for discriminating burn severity," Int. J. Appl. Earth Obs. Geoinformation 50, 170–175 (2016).
[14] Amos, C., Petropoulos, G. P. and Ferentinos, K. P., "Determining the use of Sentinel-2A MSI for wildfire burning & severity detection," Int. J. Remote Sens. 40(3), 905–930 (2019).
[15] Roteta, E., Bastarrika, A., Padilla, M., Storm, T. and Chuvieco, E., "Development of a Sentinel-2 burned area algorithm: Generation of a small fire database for sub-Saharan Africa," Remote Sens. Environ. 222, 1–17 (2019).
[16] Tompoulidou, M., Stefanidou, A., Grigoriadis, D., Dragozi, E., Stavrakoudis, D. and Gitas, I. Z., "The Greek National Observatory of Forest Fires (NOFFi)," Proc SPIE 9688 9688, 96880N-96880N – 9, Cyprus (2016).
[17] Drusch, M., Del Bello, U., Carlier, S., Colin, O., Fernandez, V., Gascon, F., Hoersch, B., Isola, C., Laberinti, P., Martimort, P., Meygret, A., Spoto, F., Sy, O., Marchese, F. and Bargellini, P., "Sentinel-2: ESA's Optical High-Resolution Mission for GMES Operational Services," Remote Sens. Environ. 120, 25–36 (2012).
[18] Gascon, F., Bouzinac, C., Thépaut, O., Jung, M., Francesconi, B., Louis, J., Lonjou, V., Lafrance, B., Massera, S., Gaudel-Vacaresse, A., Languille, F., Alhammoud, B., Viallefont, F., Pflug, B., Bieniarz, J., Clerc, S., Pessiot, L., Trémas, T., Cadau, E., et al., "Copernicus Sentinel-2A Calibration and Products Validation Status," Remote Sens. 9(6), 584 (2017).
[19] Blaschke, T., Hay, G. J., Kelly, M., Lang, S., Hofmann, P., Addink, E., Queiroz Feitosa, R., van der Meer, F., van der Werff, H., van Coillie, F. and Tiede, D., "Geographic Object-Based Image Analysis – Towards a new paradigm," ISPRS J. Photogramm. Remote Sens. 87, 180–191 (2014).
[20] Vedaldi, A. and Soatto, S., "Quick Shift and Kernel Methods for Mode Seeking," Comput. Vis. – ECCV 2008, D. Forsyth, P. Torr, and A. Zisserman, Eds., 705–718, Springer Berlin Heidelberg (2008).
[21] Cheng, Y., "Mean shift, mode seeking, and clustering," IEEE Trans. Pattern Anal. Mach. Intell. 17(8), 790–799 (1995).
[22] Rouse, J. W., Jr., Haas, R. H., Schell, J. A. and Deering, D. W., "Monitoring Vegetation Systems in the Great Plains with ERTS," Third Earth Resour. Technol. Satell.-1 Symp. NASA SP-351, S. C. Freden, E. P. Mercanti, and M. A. Becker, Eds., 309–313, NASA Special Publication, Washington, D.C. (1974).
[23] Qi, J., Chehbouni, A., Huete, A. R., Kerr, Y. H. and Sorooshian, S., "A modified soil adjusted vegetation index," Remote Sens. Environ. 48(2), 119–126 (1994).
[24] Smith, A. M. S., Wooster, M. J., Drake, N. A., Dipotso, F. M., Falkowski, M. J. and Hudak, A. T., "Testing the potential of multi-spectral remote sensing for retrospectively estimating fire severity in African Savannahs," Remote Sens. Environ. 97(1), 92–115 (2005).
[25] Trigg, S. and Flasse, S., "An evaluation of different bi-spectral spaces for discriminating burned shrub-savannah," Int. J. Remote Sens. 22(13), 2641–2647 (2001).
[26] Key, C. H. and Benson, N. C., "Landscape Assessment: Ground measure of severity, the Composite Burn Index; and Remote sensing of severity, the Normalized Burn Ratio," Other Government Series RMRS-GTR-164-CD: LA 1-51, USDA Forest Service, Rocky Mountain Research Station, Ogden, UT (2006).
[27] USGS., "Landsat Surface Reflectance-derived Spectral Indices," Product Guide Version 3.5, Department of the Interior, U.S. Geological Survey (2017).
[28] Hardisky, M. A., Klemas, V. and Smart, R. M., "The Influence of Soil Salinity Growth Form and Leaf Moisture on the Spectral Radiance of Spartina alterniflora Canopies," Photogramm. Eng. Remote Sens. 49(1), 77–83 (1983).
[29] Xu, H., "Modification of normalised difference water index (NDWI) to enhance open water features in remotely sensed imagery," Int. J. Remote Sens. 27(14), 3025–3033 (2006).
[30] Moustakidis, S. P., Theocharis, J. B. and Giakas, G., "Feature selection based on a fuzzy complementary criterion: application to gait recognition using ground reaction forces," Comput. Methods Biomech. Biomed. Engin. 15(6), 627–644 (2011).
[31] Vapnik, V. N., [Statistical learning theory], Wiley, New York (1998).
[32] Fawcett, T., "An introduction to ROC analysis," Pattern Recognit. Lett. 27(8), 861–874 (2006).